Int. J. Rock Mech. Min. Sci. & Geomech. Abstr. Vol. 21, No. 2, pp. 63–73, 1984
Printed in Great Britain. All rights reserved

0148-9062/84 $3.00 + 0.00

The Time-dependent Strain Relaxation of Algerie Granite

T. ENGELDER*

In situ *measurements of both instantaneous and time-dependent relaxation of the Algerie granite at a quarry near East Otis, Massachusetts, indicate that the orientation of instantaneous maximum expansion is 30° different from the orientation of the time-dependent maximum expansion. Based on comparison of these measurements with the regional contemporary tectonic stress and with measurements of petrofabrics of the sampled unit, it appears that the instantaneous relaxation orientation (ENE) is controlled by contemporary tectonic stress, whereas the time-dependent relaxation orientation is controlled by healed microcracks in the granite. The curves for time-dependent relaxation best fit a power-law function of time with the exponent varying between 0.211 and 0.872.*

INTRODUCTION

Inelastic or time-dependent creep commonly follows elastic strain when polycrystalline materials including rocks are subjected to stresses that are maintained at less than 10^{-5} of their shear modulus at temperatures less than half their melting temperature [1]. Laboratory experiments show that rocks exhibit an analogous behaviour when stresses are removed [2]. This behaviour involves both an instantaneous expansion and a time-dependent expansion. Examples of the time-dependent expansion upon unloading include excavations of the Niagara hydroelectric power project, Ontario, Canada, where walls of the power station are known to have expanded inward over extended periods of time [3] and continued expansion of cores from deep wells [4,5]. Two poorly understood aspects of time-dependent expansion after unloading are the mechanisms causing this behaviour and the relation between the time-dependent expansion and the *in situ* stress conditions.

Despite some work on the problem, the mechanism for inelastic creep in rocks following both loading and unloading remains elusive. First, it is not entirely clear that the mechanisms are the same for loading and unloading. Carter and Kirby [6] suggest that the low temperature inelasticity of rocks may be associated with the interaction of the applied stresses and pre-existing cracks. Varnes and Lee [7] equate the time-dependent relaxation of rocks (inelastic creep) with the mobilization of residual stress. Varnes and Lee's model includes a series of springs which may represent either microcracks or the elastic strain of grains and cement in rocks. Exactly how the microcracks or strained aggregate relax with time after unloading is not clear. However, measurements of core expansion after drilling such as those by Swolfs [4] and Teufel [5] show strain–time characteristics similar to those predicted by Varnes and Lee [7] for unloading and observed by many including Carter and Kirby [6] for loading.

If there is a relation between the *in situ* stress conditions and the time-dependent relaxation of cores, then stress may be inferred without making a direct *in situ* measurement [8]. Some workers have measured the time-dependent (inelastic) relaxation of rock cores as they are removed from a deep well and subsequently used the principal strains from the time-dependent relaxation as an indication of the direction for propagation of hydraulic fracture [4,5]. This scheme is based on Voight's [9] suggestion that *in situ* stress can be calculated directly from the time-dependent relaxation of rocks. Several experiments showing the creep-recovery of rock upon removal of stress [2] were cited as the empirical justification for considering the recovered time-dependent strain to be proportional to the total recoverable strain in rheologically isotropic rocks. These rocks, however, were loaded over short periods in the laboratory. To date, little data exist on the relations among the time-dependent relaxation, rock fabric, and instantaneous relaxation for cores subject to long-term *in situ* loads of the earth [10]. In Teufel's experiment different transducers were used to measure the instantaneous and time-dependent relaxation.

To test for factors that may control the orientations of instantaneous and time-dependent strain relaxation, the standard doorstopper overcoring set-up used for strain relaxation measurements was modified. The doorstoppers strain gauges are attached to a computer-motivated multiplexer which can sample strain gauges at set time intervals both during and after the drilling.

TECHNIQUES

For each measurement, a doorstopper module (see description of the module in Sbar *et al.* [11]) was bonded

* Lamont-Doherty Geological Observatory of Columbia University, Palisades, NY 10964, U.S.A.

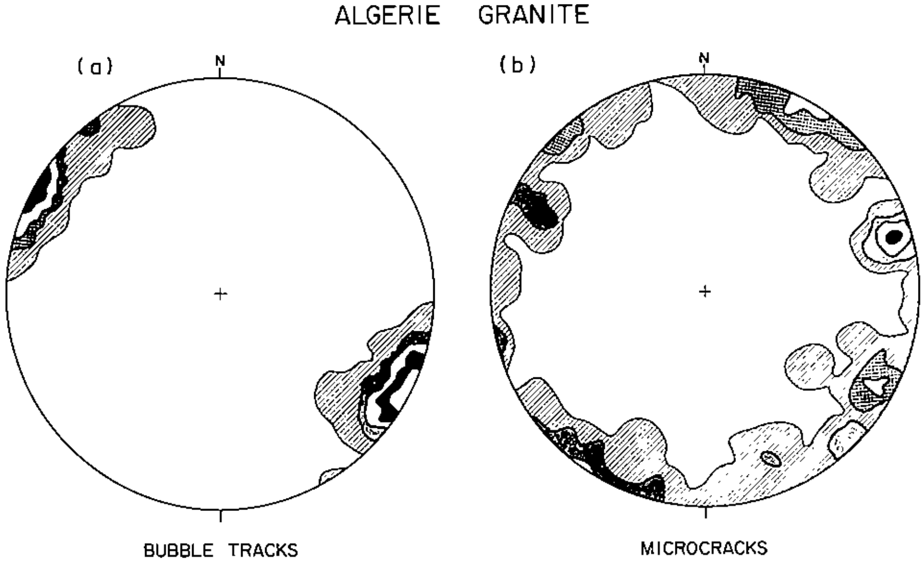

Fig. 3. Lower hemisphere projection of poles to: (a) healed microcracks and (b) open microcracks in the Algerie granite. Contours represent 2% per 1% area.

TEMPERATURE RECORD

One doorstopper was bonded about 10 cm above the sheet fracture and monitored through a period of 15 hr during which the ambient air temperature dropped from 32 to 21°C and rain plus groundwater run-off filled an initially dry hole. A perfectly compensated doorstopper bonded to a free block should show no strain during this thermal change; but the Barre granite thermal compensation chip embedded within the doorstoppers do not have exactly the same thermal expansivity as the Algerie granite; the difference is about 1 part in 30, with both rocks having a thermal expansivity of about 6.5 $\mu\epsilon$ per °C. The rock temperature at the botton of the borehole dropped from 19.4 to 12.8°C during this period. Yet, all three strain components showed an apparent tendency to expand (Fig. 4) which, in fact, is the result of the compensation chip contracting more than the Algerie granite. The significance of this behaviour will be discussed in relation to the state of stress within the granite quarry.

At the Williams Quarry the initial rock temperature varied among six experiments from 11.9 to 15.8°C (Fig. 5). This is in sharp contrast to the temperatures as high as 25°C reported during August 1969 at 1 m depth in the Mount Airy Granite, North Carolina [15]. The difference between the two quarries is that the Massachusetts quarry was not subject to the same extreme summer temperature, and the presence of circulating groundwater in the Williams quarry served to keep the rock temperature closer to that of rock at depths greater than 25 m. The range in temperature may reflect the difference in ambient air temperature which was different during different experiments, or it may reflect a difference in thermistors. It is doubtful that the rock temperature at 1 m depth increased 3.9°C during the 4-day interval between experiments 3 and 11.

The temperature record is shown for several experiments in Fig. 5. All curves have similar characteristics. Water, heated in the drilling fluid circulation hose, caused an increase in temperature as water was initially circulated through the drill and onto the doorstopper. Recovery from this thermal spike occurred as soon as cool groundwater from the pool at the bottom of the quarry reached the doorstopper. The groundwater used for clearing the drill bit rarely had exactly the same temperature as the water and rock in the borehole prior to drilling, but in a majority of cases the difference was negligible by the onset of drilling. After drilling was stopped, the temperature in the borehole stabilized although not necessarily at the exact temperature as that at the start of the experiment.

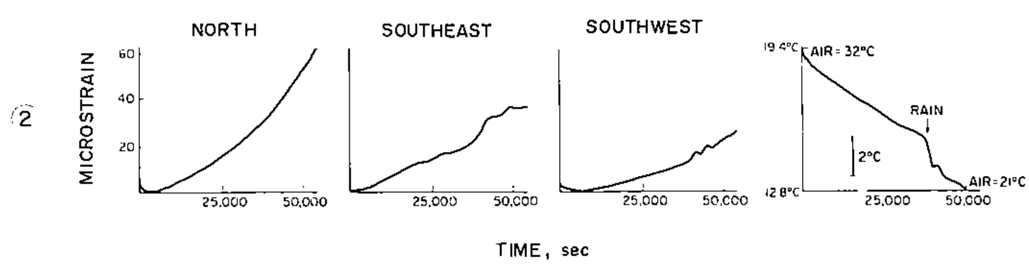

Fig. 4. Strain (expansion) vs time curves recording the behaviour of Algerie granite during a thermal change prior to overcoring for experiment 2. The components of the doorstopper are listed as the north, southeast and southwest strain gauges respectively. A temperature vs time curve is also shown for this same time interval.

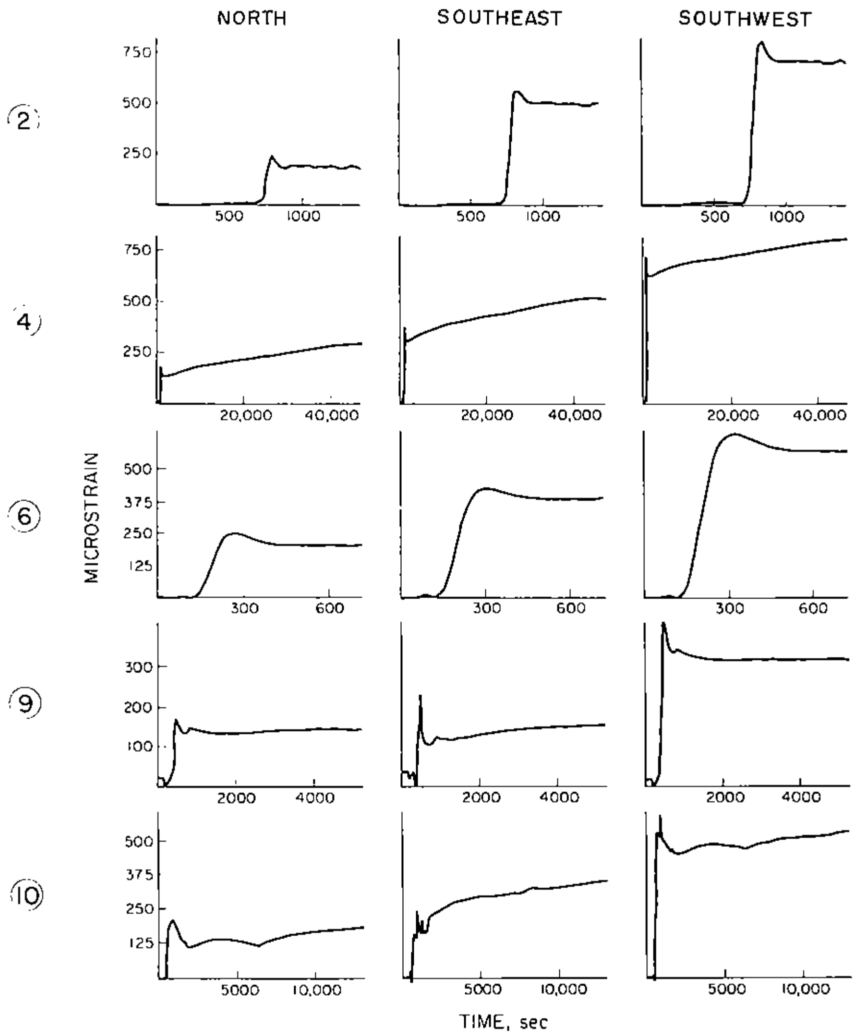

Fig. 7. Strain (expansion) vs time curves recording the behaviour of Algerie granite during and after overcoring for experiments 2, 4, 6, 9 and 10.

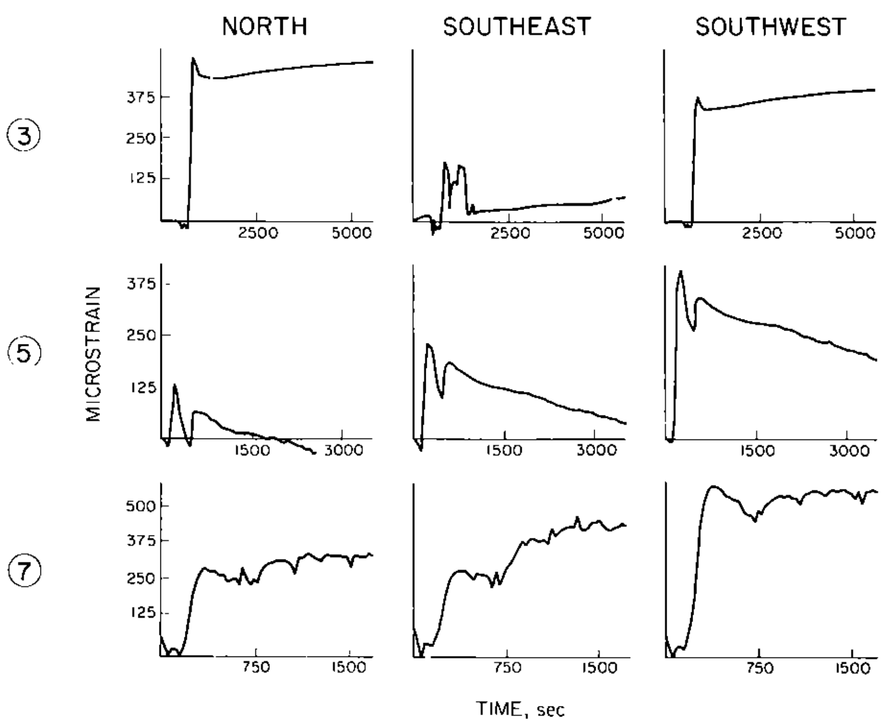

Fig. 8. Strain (expansion) vs time curves for which the behaviour is believed due to improper construction or installation of the doorstopper. Experiments are 3, 5 and 7.

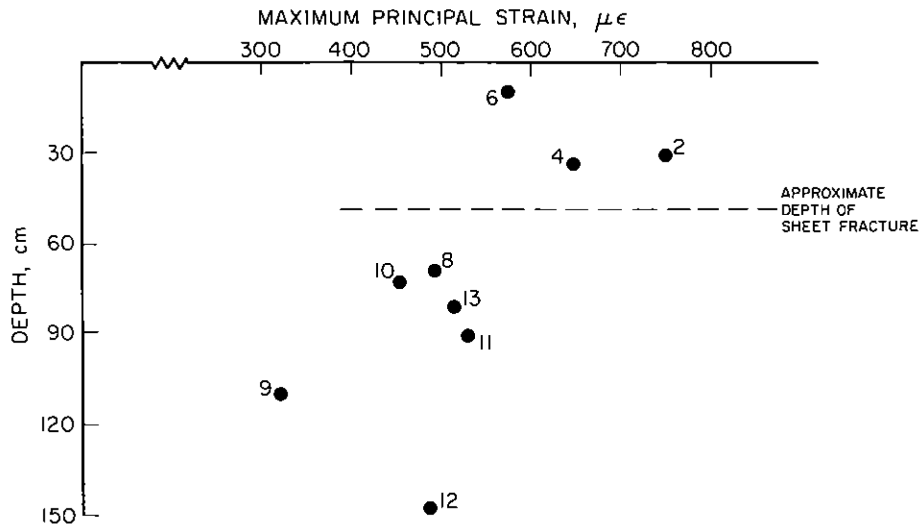

Fig. 10. A plot of maximum expansion for instantaneous relaxation vs depth of doorstopper.

magnitude of the peak minus the instantaneous strain (Poisson expansion) vs the instantaneous strain is given in Table 1 and, as predicted by Wong and Walsh's [17] calculations, the southwest component with the maximum relaxation showed the minimum ratio of Poisson expansion to instantaneous strain relaxation.

Instantaneous relaxation

Table 2 gives the principal components of the instantaneous relaxation and the orientation of the maximum component. The magnitude of the maximum principal component varies by a factor of two with the measurements above the sheet fracture showing higher values. The orientation of the maximum expansion is ENE within a range of 26°.

The Algerie granite has a compressibility (pseudolinear compressibility of Sbar *et al.* [11]) of 2×10^{-5} MPa^{-1} with an anisotropy of 4% more compressibility in the east–west direction. Taking the average instantaneous strain relief below the sheet fracture, a differential stress of 19.3 MPa is calculated. This is compatible with the New England quarrymen's motion that quarries within the Algerie granite 'contain high stress'.

Time-dependent relaxation

The time-dependent portion of the strain relaxation curves for experiments 4, 8, 10, 11, 12 and 13 have been expanded to show a relaxation that increases at a decreasing rate with time (Fig. 9). In comparing the relative magnitudes of the three components of each experiment the north component is generally less than the other two which are about equal. This contrasts with the instantaneous relaxation where the southwest component was consistently the largest of the three.

DISCUSSION

Environmental controls on relaxation behaviour

In interpreting the time-dependent relaxation of the Algerie granite as a behaviour inherent to the granite rather than the response of the granite to a change in temperature or moisture environment, one must assume that the granite was saturated prior to drilling. For the samples above the sheet fracture (2, 4 and 6) this is not a good assumption. Rock along the sheet fracture was wet but groundwater flowed along the fracture only after a rain. The surface of the granite was dry between rain and obviously offered the opportunity for the upper 45 cm of the granite to dry. Moisture along the sheet fracture suggests that even during the driest part of the year the granite below the sheet fracture remained saturated. By starting with a saturated rock below the water table and by cooling the drill bit with groundwater at the temperature of the rock, the environmental effects on the time-dependent relaxation of rocks have been minimized. During the period after overcoring, the temperature changes are small enough as to produce only a fraction of the thermal expansion observed during the time-dependent relaxation. Likewise a rock sample saturated by virtue of being below the water table will not be affected by the expansion and contraction of wetting and drying [18].

Strain above the sheet fracture

Moisture or surface temperature, however, may have affected the magnitude of the instantaneous relaxation as indicated by a plot of strain with depth where the near-surface strain was greater than strain at depth (Fig. 10). Because this strain–depth curve resembles that shown in Sbar *et al.* [19] for the vicinity of the San Andreas fault, it can be inferred that increased rock temperature above the sheet fracture could be one source of the largest instantaneous strain relaxation in the top 45 cm of Algerie granite.

The granite above the sheet fracture could also be treated as a buckled plate [10 × 10 m × 45 cm thick] pinned at steps east and west of the drill site. Using a modulus of 0.5×10^5 MPa for the Algerie granite, the critical buckling stress for such a sheet is on the order of 20 MPa, a value close to that found within the Algerie granite. The buckled plate is pinned with a radius of

Hence, it can be inferred that the instantaneous relaxation below the sheet fracture reflects a basic expansion accompanying the release of the contemporary stress field. However, the orientation of the instantaneous relaxation above the sheet fracture may reflect in part the east–west compression of the buckled plate.

An orientation of instantaneous relaxation may also be predicted from the thermal strain recorded during experiment 2 (Fig. 4). Using a thermal expansivity of 6.5 μm per °C and a temperature change of 6.6°C the free contraction of the granite should have been 43 μm in all directions. The Algerie granite has an anisotropy in thermal expansivity of less than 1 part in 25. A free contraction should have been compensated by the half bridge within the doorstopper. Yet, the data in Fig. 4 show that the *in situ* granite did not contract as much as the compensation chip embedded within the doorstopper. It appear that the granite was compressed in the east–west direction because cooling of the granite resulted in contraction in the east–west direction at a rate less than the thermal contraction of an unloaded sample. It also appears that the granite was constrained by rigid boundaries in the orthogonal direction because there was very little strain in that direction. From these values an orientation of maximum compressive strain within the Algerie granite is N80°E or within 10° of the compression buckling the sheet (Fig. 11).

The maximum expansion direction of the time-dependent relaxation is subparallel to the normal to healed microcracks in the granite (Fig. 3). Because the maximum expansion is normal to the healed microcracks, it is reasonable to hypothesize that the time-dependent relaxation is nothing more than the slow opening of these microcracks. But, the healed microcracks actually consist of fluid-filled bubble tracks, with each bubble being a sphere and unlikely to expand in a preferred orientation. Yet, the microcrack fillings must in some manner recrack in their original planes because expansion operates normal to the bubble tracks. Despite the correlation between time-dependent relaxation and bubble tracks, the processes associated with the time-dependent relaxation still remain obscure, particularly as it might pertain to the mobilization of residual stress. Open microcracks in the granite form a diffuse pattern with a weak maximum toward the ENE that does not appear to be related to time-dependent relaxation orientation (Fig. 3).

It has been suggested that open microcracks are coaxial with the *in situ* stress field [27, 5]. In particular, the assumption is made that microcracks are induced in the core as the rock expands instantaneously upon release from *in situ* stresses and that the cracks continue to open in a time-dependent manner[28]. In the Algerie granite, evidence for instantaneous microcracking may be seen in the orientation of open microcracks which have a weak maxima in the direction normal to the direction of the instantaneous maximum expansion. However, unlike the behaviour reported in Teufel [5], a second microcrack set appears to be activated during the time-dependent relaxation.

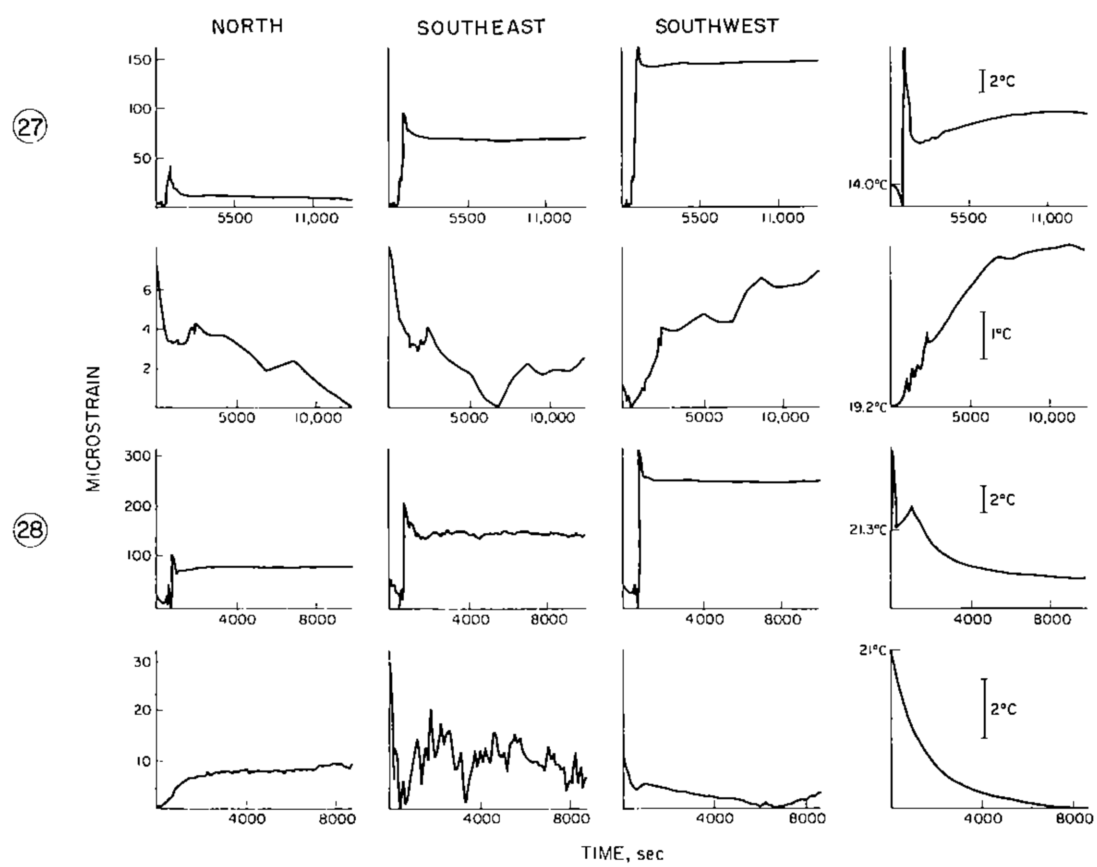

Fig. 12. Strain (expansion) vs time curves for the total relaxation and time-dependent relaxation of the Onondaga limestone for experiments 27 and 28.

seismicity in eastern North America: An example of intra-plate tectonics. *Geol. Soc. Am. Bull.* **84,** 1861–1882 (1973).

24. Haimson B. C. Crustal stress in the continental U.S. as derived from hydraulic fracturing measurements. In *The Earth's Crust,* Geophysical Monograph No. 20 (Edited by J. G. Hickock), pp. 576–592. AGU, Washington, DC (1977).
25. Zoback M. L. and Zoback M. State of stress in the conterminous United States. *J. geophys. Res.* **85,** 6113–6156 (1980).
26. Engelder T. Is there a genetic relationship between selected regional joints and contemporary stress within the lithosphere of North America? *Tectonics* **1,** 161–177 (1982).
27. Strickland F. G. and Ren N. K. Predicting the *in-situ* stress for deep wells using differential strain curve analysis. SPE/DOE 8954, pp. 251–255 (1980).
28. Engelder T. and Plumb R. Changes in *in situ* ultrasonic properties of rock on strain relaxation. *Int. J. Rock Mech. Min. Sci. & Geomech. Abstr.* **21,** 75–82 (1984).
29. Engelder T. and Geiser P. Near surface *in-situ* stress: Part IV. Residual stress in the Tully limestone, Appalachian plateau, New York. *J. geophys. Res.* (1984). In press.
30. Swolfs H. S., Lingle R. and Thomas J. M. Strain-relaxation tests on selected cores from El Paso Natural Gas Well Largo Canyon No. 288. Technical Rept 76–50, Terra Tek, Salt Lake City, UT, 23 pp (1976).

Table 4. Parameters for time-dependent relaxation, $\epsilon = at^b$

	a	b	Coefficient of determination
El Paso Canyon Largo Well No. 256, Farmington, New Mexico Dakota sandstone			
Dakota 7039′			
Gauge 1#	4.908	0.396	0.950
Gauge 3#	1.294	0.477	0.909
Dakota 7026′			
Gauge 1#	4.528	0.448	0.968
Gauge 2#	0.897	0.535	0.982
General Crushed Stone Quarry, Geneva, New York Onondaga limestone			
Data 28			
Gauge 1#	0.734	0.338	0.840
Data 27			
Gauge 3#	0.449	0.367	0.973
Data 29			
Gauge 1#	0.215	0.612	0.980
Gauge 2#	0.661	0.496	0.987
Gauge 3#	0.780	0.452	0.968

Comparison with other results

The Onondaga limestone near Geneva, New York, was also tested for time-dependent strain relaxation [29]. Relaxation curves from the Onondaga limestone show little or no tendency to expand with time after overcoring (Fig. 12). At the test site the Onondaga limestone was cut by steeply inclined fractures spaced at 10–50 cm and so there is a possibility that the process of jointing relieved much of the time-dependent strain. Other examples of time-dependent expansion include those reported by Swolfs [4] on the Dakota sandstone from the El Paso Canyon Largo Well No. 256, Farmington, New Mexico. Using the iterative technique for calculation of a power of time for some of Swolfs' data, it is apparent that the Dakota sandstone behaves in the same manner as the granite (Table 4). For the Dakota sandstone, the correlation coefficient is less than for the Algerie granite primarily because of the larger amount of time between the cutting of the core and the initial recording of the time-dependent relaxation (3 hr vs 5 min). Swolfs *et al.* [30] also reports that time-dependent strain was not found in another well (Canyon Largo No. 288) within the Dakota sandstone. Dense fracturing characterized the Dakota sandstone within this latter well and led Swolfs to suggest that the process of fracturing relieved the time-dependent strain.

CONCLUSIONS

Near-surface bedrock can exhibit both instantaneous (elastic) and time-dependent (inelastic) strain relaxation when overcored. At our experimental site, it appears that the elastic component reflects the contemporary tectonic stress field, whereas the time-dependent component, which obeys a power law, is related to the opening of healed microcracks. The two components are not parallel and thus, measurement of one cannot be used to predict the orientation of the other.

Acknowledgements—I thank Ted Koczynski for helping me design the multiplexer to interface strain gauge bridges with the Hewlett–Packard calculator system. Steve Marshak and Steve Brown helped with the field experiments. Ed Williams was very gracious in giving my field experimenters free access to the Williams Stone Company quarry in East Otis, Massachusetts. Early versions of this paper were read by Steve Marshak, Tracy Johnson and Chris Scholz. This work was supported by contracts from the Nuclear Regulatory Commission (NRC-04-81-180) and the New York State ERDA. Lamont-Doherty Geological Observatory Contribution No. 3587.

Received 20 *May* 1983; *revised* 14 *October* 1983.

REFERENCES

1. Weertman J. and Weertman J. R. Mechanical properties, strongly temperature dependent. In *Physical Metallurgy* (Edited by Cahn R. W.), pp. 983–1010 (1970).
2. Robertson E. C. Viscoelasticity of rocks. In *State and Stress in the Earth's Crust* (Edited by Judd W.), pp. 181–224. Conference, Santa Monica (1964).
3. Lee C. F. and Lo K. Y. Rock squeeze study of two deep excavations at Niagara Falls. *Proc. ASCE Speciality Conf. on Rock Engineering*, Boulder, CO, pp. 116–140 (1976).
4. Swolfs H. S. Determination of *in-situ* stress orientation in a deep gas well by strain relief techniques. Technical Rept 75–43, Terra Tek, Salt Lake City, UT, 47pp (1975).
5. Teufel L. W. Determination of *in-situ* stress from anelastic strain recovery measurements of oriented core. *SPE/DOE Symp. on Low Permeability*, Denver, CO, SPE/DOE 11649, pp. 421–430 (1983).
6. Carter N. L. and Kirby S. H. Transient creep and semibrittle behavior of crystalline rocks. *PAGEOPH* **116**, 807–839 (1978).
7. Varnes D. J. and Lee R. T. hypothesis of mobilization of residual stress in rock. *Geol. Soc. Am. Bull.* **83**, 2863–2866 (1972).
8. Blanton T. L. The relation between recovery deformation and *in-situ* stress magnitude. *SPE/DOE Symp. on Low Permeability*, Denver, CO, SPE/DOE 11624, pp. 213–218 (1983).
9. Voight B. Determination of the virgin state of stress in the vicinity of a borehole from measurements of partial anelastic strain tensor in drill cores. *Rock Mech. Engng Geol.* **6**, 210–215 (1968).
10. Teufel L. W. Prediction of hydraulic fracture azimuth from anelastic strain recovery measurements of oriented core. In *23rd U.S. Natn Rock Mechanics Symp.*, Berkeley, CA, pp. 238–245 (1982).
11. Sbar M. L., Engelder T. and Marshak S. Stress pattern near the San Andreas fault, Palmdale, California, from near-surface *in-situ* measurements. *J. geophys. Res.* **84**, 156–164 (1979).
12. Ratcliffe N. M. (Ed.) Cross section of the Berkshire Massif at 42°N: profile of a basement reactivation zone. In *Guidebook for Field Trips in Western Massachusetts and Adjacent Areas, NEIGC, 67th Annual Meeting*, pp. 186–219. City College of CUNY, New York (1975).
13. Dale T. N. The commercial granites of New England. *U.S. Geol. Surv. Bull.* **738**, 488pp (1923).
14. Plumb R. A., Engelder T. and Yale D. Near surface *in-situ* stress: Part III. Microcrack fabric within the New Hampshire granites. *J. geophys. Res.* (1984). In press.
15. Hooker V. E. and Duvall W. I. *In-situ* rock temperature: stress investigations in rock quarries. USBM RI 7589, 12pp (1971).
16. Hooker V. E. and Bickell D. L. Overcoring equipment and techniques used in rock stress determination. USBM IC 8618, 32pp (1974).
17. Wong T. F. and Walsh J. B. Theoretical analysis of tectonic stress relief during overcoring. Preprint (1982).
18. Savage W. Z. A model of the strain response of Barre granite to setting and drying. *U.S. Geol. Surv. Open-file Rept* 79-768, 17pp (1979).
19. Sbar M. L., Richardson R. M., Flaccus C. and Engelder T. Near surface *in-situ* stress: Part I. Strain relaxation measurements along the San Andreas fault in southern California. *J. geophys. Res.* (1984). In press.
20. Johnson A. M. *Physical Processes in Geology*, 577pp. Freeman, San Francisco (1970).
21. Murrell S. A. F. Rheology of the lithosphere-experimental indications. *Tectonophysics* **36**, 5–24 (1976).
22. Goetze C. and Brace W. F. Laboratory observations of high-temperature rheology of rocks. *Tectonophysics* **13**, 586–600 (1972).
23. Sbar M. L. and Sykes L. R. Contemporary compressive stress and

curvature of 2.5×10^5 cm. This shape imparts a maximum fibre strain [20] of about 180 $\mu\epsilon$. Within the buckled sheet, the relative magnitudes of measurements 2 and 4 suggest they were made below the neutral fibre and whereas, measurement 6 was made above the neutral fibre.

Inelastic creep

The time-dependent relaxation curves of Fig. 9 can be fit by a power law curve where strain varies as a power of time. An iterative technique for curve fitting was necessary because the record for time-dependent strain did not begin immediately upon initiation of drilling. The first and largest part of the time-dependent relaxation is swamped by the instantaneous relaxation. The iterative technique gives a best estimate for the total strain released by a time-dependent mechanism. The curve selected by the iterative technique was that with the best coefficient of determination (Table 3). The power of time varies from 0.211 in experiment 8 to 0.872 in experiment 11. A power of 0.2 gives a total time-dependent relaxation much less than the instantaneous relaxation whereas a power of 0.8 gives a time-dependent relaxation much more than the instantaneous relaxation. The magnitudes of the time-dependent strain at 10,000 sec (3 hr) and 100,000 sec (30 hr) have been calculated and from these values the principal strains and their orientations are plotted (Fig. 11). In general the maximum principal axis of the time-dependent relaxation has a more east–west trend than the instantaneous relaxation.

One transient creep law for rocks has the same form as the time-dependent relaxation curves which we recorded [6]:

$$\epsilon = at^b$$

This creep law best fits the behaviour of transient creep at low strain (less than 10^{-2}) when rocks have been

Table 3. Parameters for time-dependent relaxation, $\epsilon = at^b$

Test	a	b	Coefficient of determination
4-N	0.698	0.518	0.998
4-SE	0.284	0.630	0.999
4-SW	0.439	0.573	0.998
8-N	0.480	0.478	0.987
8-SE	0.533	0.475	0.964
8-SW	8.029	0.231	0.989
10-N	0.113	0.714	0.993
10-SE	3.101	0.429	0.953
10-SW	0.098	0.739	0.997
11-N	0.023	0.872	0.994
11-SE	0.032	0.871	0.999
11-SW	0.074	0.789	0.997
12-N	0.130	0.713	0.999
12-SW	0.602	0.577	0.997
12-SE	0.446	0.602	0.999
13-N	14.809	0.211	0.999
13-SW	4.323	0.359	0.999
13-SE	3.482	0.386	0.999

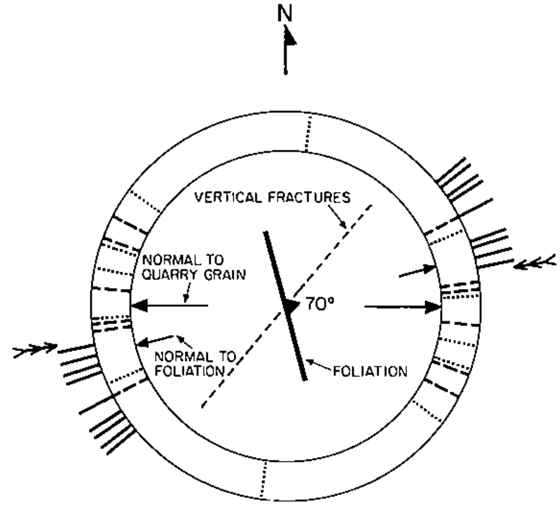

Fig. 11. A plot of the orientation of maximum expansion for both instantaneous and time-dependent relaxation of Algerie granite.

subject to uniaxial compression [21] or triaxial compression [22]. Carter and Kirby [6] suggest that the power-law transient creep equation is not particularly appropriate for loading tests where steady-state creep may also contribute to the total strain during the period of transient behaviour. This criticism is not applicable to relaxation tests where steady-state creep does not contribute to the total strain. Because the loading and unloading curves have the same form, it is reasonable to hypothesize that the same deformation mechanisms operate during both.

A power law for time-dependent strain relaxation of Algerie granite is tenuous because the value for the power of time established from six tests varies more than the values reported in Carter and Kirby [6] for the loading of several different rock types from several different laboratories. Too little data on the time-dependent relaxation of rock is available to know whether this scatter in power of time is common for rocks *in situ* or inherent in the experimental technique.

Mechanisms of strain relaxation

The mean for the orientation of the maximum expansion of the instantaneous relaxation is N64°E and, thus is oriented about 30° counterclockwise from the mean for the time-dependent component of relaxation (Fig. 11). Neither the time-dependent nor the instantaneous relaxation orientations appear to be related to the nearby vertical joints in the floor of the quarry nor, for that matter, the geometry of the quarry where the nearest walls are oriented east–west. The instantaneous relaxation (N64°E) is nearly parallel with the well documented ENE maximum principal contemporary tectonic stress in the northeastern United States [23–26]. This latter correlation is made credible by data indicating that contemporary tectonic stress can be detected near the surface in the vicinity of the San Andreas fault [19].

Table 1. Poisson expansion vs instantaneous relaxation

Test	Component North	Southeast	Southwest
2	0.340	0.125	0.126
4	0.314	0.206	0.135
6	0.241	0.125	0.135
8	0.139	0.136	0.137
11	0.174	0.219	0.118
12	0.282	0.135	0.132
13	0.194	0.250	0.132

Table 2. Instantaneous relaxation

Test	Depth (cm)	$\mu\epsilon_{max}$	$\mu\epsilon_{min}$	Azimuth ϵ_{max}
2	31	751	154	78
4	33	648	60	70
6	10	598	171	75
8	69	495	247	57
9	109	320	10	55
10	73	455	44	62
11	90	529	93	52
12	147	488	98	72
13	81	515	110	52

about 500 $\mu\epsilon$ whereas the other two components were not consistent. Curves of good to intermediate quality are shown for experiments 2, 4, 6, 9 and 10 where the magnitudes of the three components have the same general value and ratio to each other (Fig. 7). Curves 9 and 10 show spurious changes in slope that detracts from their overall quality. For completeness, curves from experiments 3, 5 and 7 are shown (Fig. 8) and even here the basic form of the relaxation may be seen in curves from experiments 3 and 7.

Poisson expansion

On initial cutting, the top of the core over-expands in response to the stresses normal to the axis of the core but just under the notch of the cut [16]. This is a Poisson expansion that is maximum at a cutting depth of half the radius of the core [17]. At cutting depths of about three radii, the Poisson expansion is relieved at the surface of the core and the remaining value of the strain relaxation is taken to be the maximum estimate of the instantaneous relaxation. For several experiments, a ratio of the

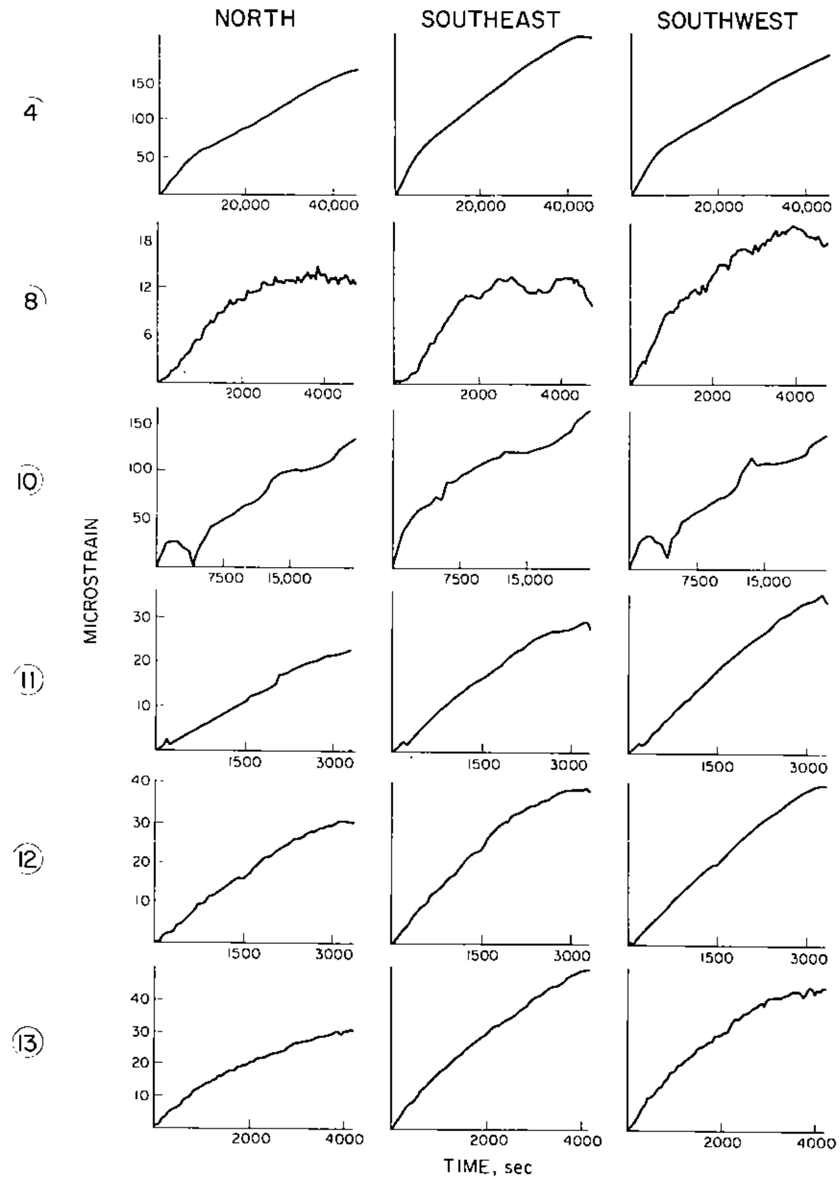

Fig. 9. Strain (expansion) vs time curves for the time-dependent relaxation of Algerie granite for experiments 4, 8, 10, 11, 12 and 13.

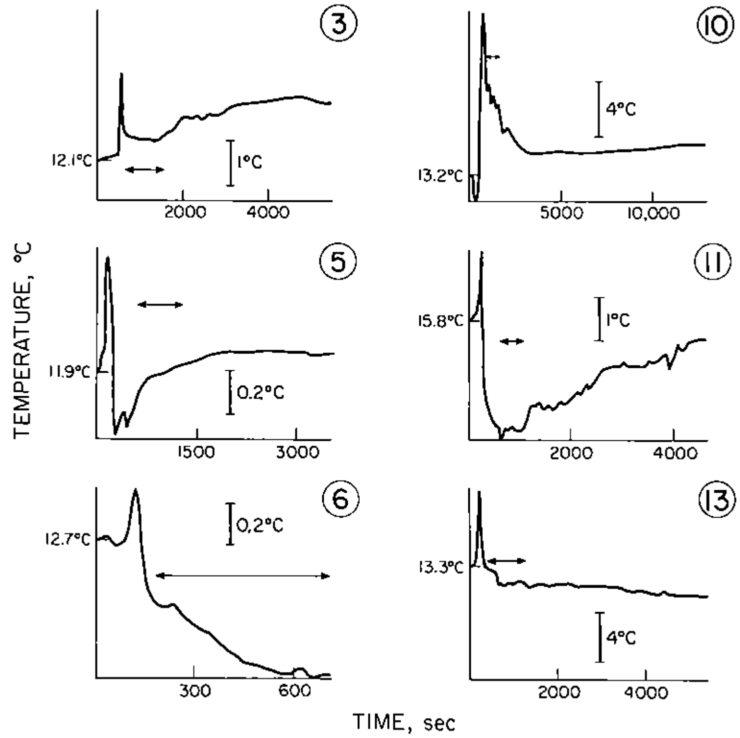

Fig. 5. Temperature vs time curves for experiments 3, 5, 6, 10, 11 and 13. the horizontal arrows indicate the period of overcoring.

RELAXATION DATA

Of the 12 overcoring experiments within the Algerie granite, relaxation curves from experiments 8, 11, 12 and 13 conform very well with the shape of an ideal strain relaxation test (Fig. 6). In all four cases, the southwest component expanded the most with an average value of

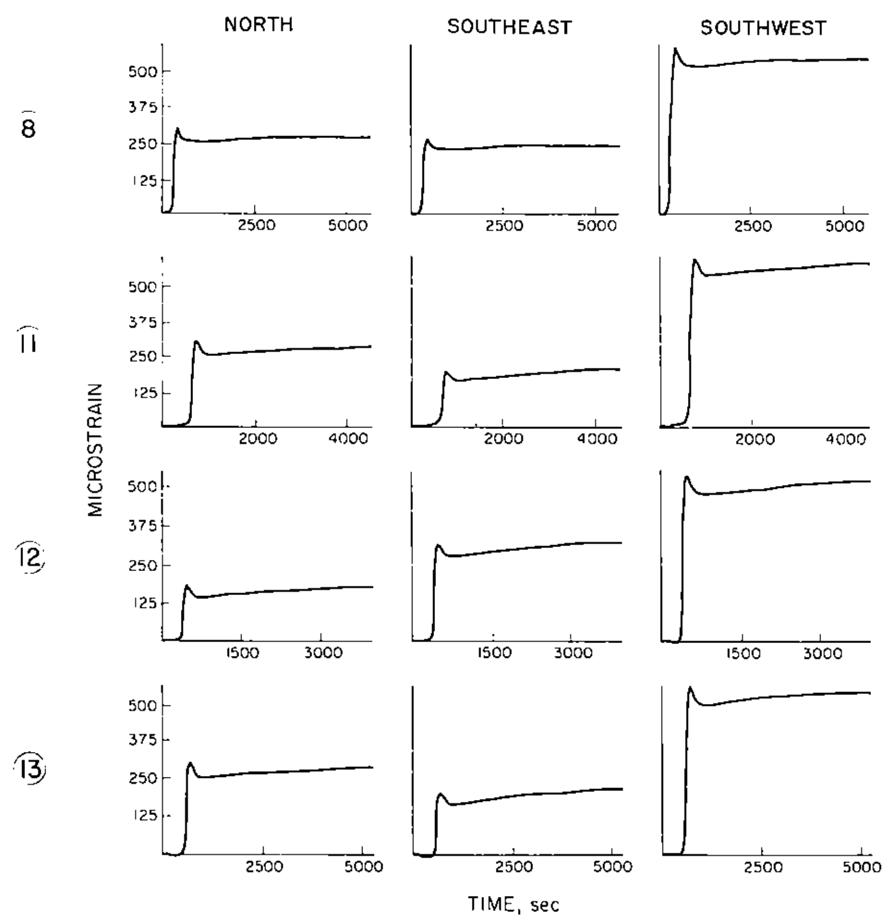

Fig. 6. Strain (expansion) vs time curves recording the behaviour of Algerie granite during and after overcoring for experiments 8, 11, 12 and 13.

to the flattened and cleaned bottom of a borehole. Our doorstoppers were modified by the addition of a 100,000 Ω thermistor whose active element was placed adjacent to the strain gauge rosette. The doorstopper module was hardwired to an electrical cable, and the cable was fed through the drill string to the surface, where it was attached to multiplexer and bridge unit designed and built at Lamont by Ted Koczynski. This unit was interfaced with a voltmeter, an HP41-CV programmable calculator, a tape drive and a printer. The multiplexer was necessary because the HP41-CV could only sample one piece of data at a time at the rate of one sample per second. We also connected a linear potentiometer, which monitored vertical displacement of the drill bit during drilling. After the epoxy, bonding the module to the rock, had set, modules were overcored to six inches. After overcoring, the drill was stopped and the bit, drill shaft, and core in the borehole were not disturbed again until the time-dependent strain relaxation measurements were terminated. The electronics automatically sampled six channels of data (three strain gauges of the doorstopper, temperature from the thermistor, bit displacement from the linear potentiometer and time) at a preset interval, stored these data on magnetic tape and printed them on a paper chart. Generally data were recorded at 30 sec intervals during drilling, and then at 5 min intervals for 2 hr after drilling or 15 min intervals for 14 hr. Upon return from the field, the data were processed on tape with a more powerful computer.

Typical strain relaxation curves show the relaxation divided into three parts: an instantaneous relaxation, a Poisson expansion and a time-dependent relaxation (Fig. 1). Often the quality of the strain relaxation measurement can be determined by the shape of this relaxation curve. Any curves that deviate from this basic shape are likely to indicate either a fractured rock near the strain gauges or poorly bonded strain gauges. Rapid changes in the environment surrounding the doorstopper may also lead to strain relaxation curves that do not match the shape shown in Fig. 1.

During the strain relaxation measurement, particular care was given to maintaining a constant environment. Of concern were the effects of both moisture and temperature. Because water was used for drilling fluid, the most desirable starting condition was for the rock to be saturated at the temperature of the drilling water. This was accomplished by bonding the doorstoppers below the water table and subsequently letting the borehole fill

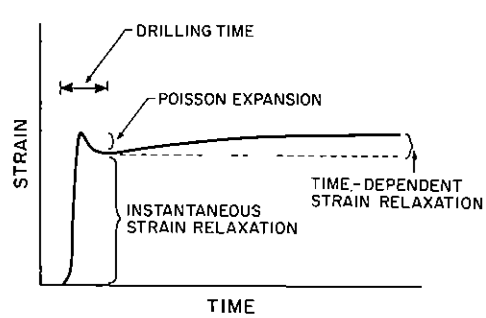

Fig. 1. A typical overcoring curve showing strain relaxation vs time.

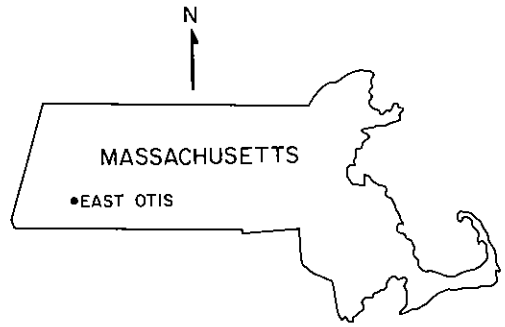

Fig. 2. Location of the Algerie granite.

with groundwater at the temperature of the rock. Water used for drilling was groundwater that was flowing into a pool at the bottom of the quarry. The temperature of this water was less than 3°C higher than the groundwater 1 m below the floor of the quarry. After drilling, the core was left in this environment to assure a time-dependent relaxation unaffected by either temperature or moisture changes.

LOCATION

All measurements discussed in this study were made in the Algerie granite exposed in the Williams Stone Company quarry near East Otis, Massachusetts (Fig. 2). The Algerie granite is a synemetamorphic quartz monzonite with a foliation striking N15°W and dipping steeply to the east. Ratcliffe [12] suggests that the granite was intruded along a major fault zone which bounds one of the crystalline nappes of the Berkshire Massif. The regional foliation of the adjacent gneisses strikes N15°W. Healed microcracks as indicated by bubble tracks within the granite have a strong preferred orientation striking about N20°E whereas open microcracks have a diffuse pattern (Fig. 3). For the Algerie granite Dale [13] reports both east–west and north–south grain planes or planes of eady splitting as used by quarrymen. The contemporary tectonic stress in the vicinity of East Otis, Massachusetts, is believed to be oriented with σ_1ENE [14].

The quarry is in the form of a 'Z' with an east–west pit connecting north–south pits extending in opposite directions from opposite ends of the east–west pit. The floor of the east–west pit is about 20 m below the surface and measures 30 m wide by 60 m long. Towards the west end of the east–west pit, there are several vertical fractures striking N40°E. Horizontal sheet fractures are spaced 50 cm apart at the surface and increase in spacing to 3 m at a depth of 20 m. Groundwater seeps out of the sheet fractures above the floor of the quarry and, hence, the quarry is occasionally pumped. The experimental site was located in the western end of the east–west pit but was not within the zone of vertical fractures. At the site, the floor of the quarry was 45 cm above a horizontal sheet fracture that the quarry owner reported propagated on release of the overburden by the quarrying operation. The next 3 m of rock below this sheet fracture was unfractured.